Soft Matter

View Online
Dynamic Article Links

Cite this: *Soft Matter*, 2011, **7**, 4742

www.rsc.org/softmatter

PAPER

Macroscopic optical effects in low concentration ferronematics

Nina Podoliak,*[a] Oleksandr Buchnev,[a] Oleksandr Buluy,[c] Giampaolo D'Alessandro,[b] Malgosia Kaczmarek,[a] Yuriy Reznikov[c] and Timothy J. Sluckin[b]

Received 13th January 2011, Accepted 9th March 2011
DOI: 10.1039/c1sm05051f

We present a detailed experimental and theoretical study of the optical response of suspensions of ferromagnetic nanoparticles ("ferroparticles") in nematic liquid crystals ("ferronematics"), concentrating on the magnetic field-induced Frederiks transition. Even extremely low ferroparticle concentrations (at a volume fraction between 2×10^{-5} and 2×10^{-4}), induce a significant additional ferronematic linear response at low magnetic field (<100 G) and a decrease in the effective magnetic Frederiks threshold. The experimental results demonstrate that our system has weak ferronematic behavior. The proposed theory takes into account the nematic diamagnetism and assumes that the effective magnetic susceptibility, induced by the nanoparticles, no longer dominates the response. The theory is in good agreement with the experimental data for the lowest concentration suspensions and predicts the main features of the more concentrated ones. The deviations observed in these cases hint at extra effects due to particle aggregation, which we have also observed directly in photographs.

1. Introduction

Liquid crystals are widely used in recording, processing and displaying information. The dielectric and diamagnetic properties of liquid crystals enable their optical properties to be controlled by applying electric or magnetic fields. Although early experimental and theoretical scientific work addressed *magnetic* reorientation, in practice most liquid crystal devices are driven by electric fields. In conventional devices, driving voltages of the order of a few volts are sufficient to trigger orientational and optical responses in liquid crystals. The low field strengths required are an attractive feature of liquid crystal technology, a fact that follows from the relatively large dielectric permittivity anisotropy in liquid crystals. By contrast, the sensitivity of nematic liquid crystals to magnetic fields is very low; the diamagnetic permeability anisotropy is approximately 10^{-7}. Thus, a rather large magnetic field (~1–10 kG) must typically be applied to elicit an analogous magnetic response in a nematic system.

In 1970, Brochard and de Gennes[1] suggested a scenario within which the sensitivity of liquid crystals to magnetic fields might be expected to increase significantly. This paper proposed that liquid crystals could be doped at very low volume concentrations by ferromagnetic particles ("ferroparticles"). They developed the first theory for these materials, and in so doing coined the term "ferronematic". In their picture, the magnetic moments of the particles in ferronematics are aligned by the external magnetic field. The coupling between the ferroparticle and the liquid crystal molecule orientations then transfers the magnetic orientational effect onto the underlying liquid crystal matrix. Ferronematics have attracted considerable interest[2–16] over the years because, in principle, they should exhibit higher magnetic susceptibilities than undoped liquid crystals, resulting in evident device applications.

The first experimental attempt to investigate ferronematic materials was carried out by Chen and Amer[2] in 1983. Their ferronematic suspensions exhibited liquid crystal orientational distortion for magnetic fields as low as a few Gauss. However, their results have not been replicated in the literature and it may be that the suspension was not stable. Furthermore, at higher external magnetic fields anomalous behavior occurred, which was thought to have been ferromagnetic particle agglomeration, but is so far not properly understood. More recently, studies of ferronematic suspensions using several different thermotropic liquid crystal matrices have been reported by Kopčanský *et al.*[11,13] They studied the orientational response in ferronematics induced not only by magnetic fields, but also by combined magnetic and electric fields. However, these experiments indicated that the magnetic Frederiks threshold can shift either up or down, depending on the liquid crystal and the nature and shape of the magnetic particles.

The Brochard–de Gennes continuum theory was first extended by Burylov and Raikher,[4,6] who studied the behavior of a single rod-like particle in the liquid crystal matrix. Supposing the liquid crystal molecules to be subject to orientational anchoring forces at the colloidal particle surface, they derived an effective

[a]*School of Physics and Astronomy, University of Southampton, Southampton, SO17 1BJ, United Kingdom. E-mail: np7g08@soton.ac.uk*
[b]*School of Mathematics, University of Southampton, Southampton, SO17 1BJ, United Kingdom*
[c]*Institute of Physics, National Academy of Sciences of Ukraine, Prospect Nauky 46, Kyiv, 03028, Ukraine*

orientational coupling between a magnetic colloidal particle and the liquid crystal molecules. In later work, they also studied the *collective* response of the suspension to an external magnetic field.[5,6] More recently, based on this work, Zadorozhnii *et al.*[12,14] made a comprehensive analysis of ferronematic properties in a magnetic field, as a function of system parameters, and in particular the effective nematic–magnetic coupling strength. The latter theory is a phenomenological theory, in which the system's magnetic response is described by two parameters: one quantifying the particle interaction with the field, and a second measuring the liquid crystal–ferroparticle torque. There are plausible links with the microscopic mechanism, but in order for this theory to hold, it does not need to specify a detailed picture of these mechanisms at all.

In several of the theoretical cases studied in detail so far , it has been supposed, following the Brochard–de Gennes hypothesis, that ferroparticle-induced effective magnetic susceptibility dominates the intrinsic magnetic susceptibility of the nematic system. In the present paper, however, this idealization no longer holds. Our model is based on the Burylov–Raikher theory. It includes both the magnetic effects associated with nematic diamagnetism, which explain the Frederiks threshold in the pure system, and the particle ferromagnetism, which induces the low field response. An analysis of the experimental data indicates that the magnetic response of the ferronematic is dominated by nematic diamagnetism. The extra effect of the ferroparticles acts as a small perturbation to this primary factor.

Our key results are that: (a) even at very low concentrations, there is an additional effect in the response of the colloidal system to the applied magnetic field in comparison with undoped nematics; (b) effects are noticeable both in the low field region, and as a shift in the effective Frederiks threshold; (c) the low field effects in particular are noticeable, even when the field on the system is only of the order of tens of Gauss; (d) even though the concentrations are low and the applied field is weak we can still detect a macroscopic change in the optical response; (e) the effect is unambiguously the consequence of the magnetic properties of the colloidal particles; (f) the results can be interpreted within a theory that explicitly supposes that the colloidal nematic also exhibits an intrinsic magnetic susceptibility.

The structure of this paper is as follows. The experimental set-up, sample preparation and results of the measurements are described in Section 2. In Section 3, we develop a phenomenological theory of ferronematics that might be expected to apply to these experiments, as discussed above. Within this section, the governing equations are developed in Subsection 3.2. In Section 4 we use the model to attempt a quantitative interpretation of some of the experimental data presented in Section 2, and also draw attention to regions where the theory is incomplete. Finally, in Section 5, we put our results in a broader context, make suggestions for further work, and draw some brief conclusions.

2. Experiment

2.1 Materials, sample preparation and experimental setup

The experiments used suspensions based on the nematic liquid crystal E7 (Merck). The principal set of ferronematic suspensions were prepared using magnetic nanoparticles made from Fe_xO_y (Sigma Aldrich). Using TEM, it was possible to determine that the ferroparticles were almost spherical, with an average diameter ~15–20 nm. A second set of suspensions were doped with α-Fe_2O_3 polydisperse nanorods (NanoAmor), with a diameter of ~40–130 nm and a length of ~250–600 nm. Both types of nanoparticle were initially dispersed in heptane, with oleic acid as a surfactant coating, to prevent aggregation of the particles. By themselves, the magnetic nanoparticles dispersed in heptane were sensitive to an external magnetic field, while the nanorods were not. The contrast in the magnetic sensitivity is not surprising; it is known[17] that at room temperature α-Fe_2O_3 exhibits only weak ferromagnetism.

In general there are two regimes for magnetic relaxation in ferrofluid systems. In the Néel regime, the moments drift around within the ferroparticles, whereas in the Brownian regime, the ferroparticles themselves rotate. In our case, a consideration of the magnetic nanoparticle size indicates that the magnetic moments are rigidly coupled to the ferroparticle crystallographic structure,[18] and the Brownian relaxation process dominates.

The nanoparticle suspension in the nematic was prepared as follows. The heptane-based dispersion of nanoparticles was added to the pure liquid crystal, mixed well, and left at an elevated temperature above 70 °C so that the solvent evaporated. Using this method, suspensions with a volume concentration of $f = 2 \times 10^{-4}$, 1×10^{-4} and 2×10^{-5} of each type of nanoparticle in liquid crystal were prepared. These concentrations correspond to interparticle distances approximately equal to 17, 22 and 34 particle diameters, respectively.

The magneto-optic response of cells filled with either pure liquid crystal or with the ferronematic suspensions was then investigated. The cells were ~50 μm thick. The cell walls consisted of glass substrates covered with a polyimide layer, with opposite walls rubbed in opposing directions. The rubbing created walls with a homogeneous in-plane liquid crystal alignment with a small pre-tilt angle of $\alpha = 2.7°$. The pre-tilt angle was measured independently by the crystal rotation method.[19]

The magneto-optic measurements were taken the day after the cells were prepared. The cell was placed between two crossed polarizers, so that the easy axis alignment directions and the polarizer directions were out of phase by an angle of $\pi/4$, as

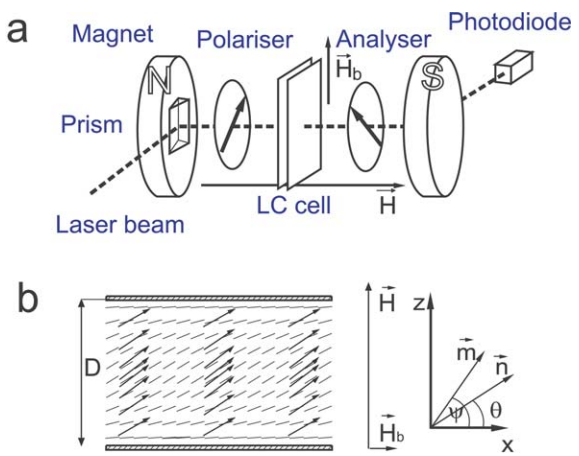

Fig. 1 (a) A schematic of the complete experimental set-up; (b) the geometry of the ferronematic cell. See text for notation.

shown in Fig. 1(a). A test magnetic field H was applied perpendicular to the cell plane. A small bias field H_b ($\simeq$20 G) in the cell plane was also imposed. This aligned the ferroparticle magnetic dipole moments at the beginning of each experimental run. Fig. 1 (b) shows the detailed liquid crystal cell geometry.

The nematic reorientation was monitored from the intensity of a laser beam passing through this optical system. The phase lag $\Delta\varphi$ induced by the liquid crystal layer could be recovered from the experimental measurements of the normalized cross-polarized intensity $I_\perp$, using the standard relation[20]

$$I_\perp = \sin^2\left(\frac{\Delta\varphi}{2}\right). \quad (1)$$

2.2 Experimental results

In Fig. 2 we plot the functional dependence of the phase lag shift on the external magnetic field for all of the systems discussed above. In the undoped liquid crystal cell there is a Frederiks threshold at $H \simeq 1.5$ kG.

However, unlike in classical Frederiks experiments,[20] here the easy-axis pre-tilt and the in-plane bias field breaks the reflection symmetry of the cell, causing the Frederiks threshold to be smeared. The smearing is increased in the colloidal suspensions, and the reorientation occurs at lower fields than for the undoped liquid crystal. This is an effect that increases with the nanoparticle volume concentration f. In addition, we note that in the ferronematic systems there is a significant additional linear effect at low fields, and this also increases with the nanoparticle concentration. This effect is much larger than the Frederiks threshold shift, in the sense that it is observable at very low magnetic fields.

We also include the results of analogous magneto-optic measurements for the α-Fe_2O_3 nanorods suspensions, see Fig. 3. Interestingly, for these weak magnetic suspensions, there is no discernible concentration dependence, nor any difference between these measurements and those in the undoped liquid crystal. The colloidal components of the two systems are matched by weight and concentration, and are made from chemically similar material, but their magnetic properties are very different. The inevitable inference is that the effects observed in the Fe_xO_y particle suspensions in Fig. 2 are due to their magnetic properties.

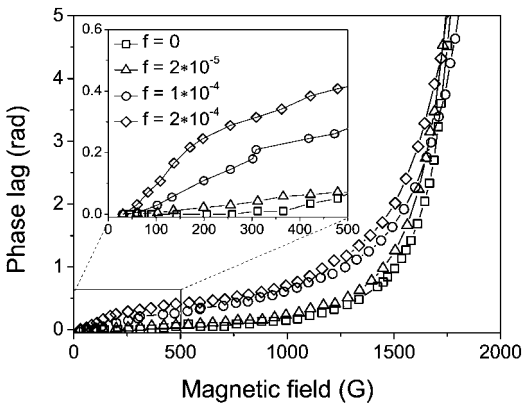

Fig. 2 The phase lag as a function of the magnetic field, for cells with pure nematic and suspensions with magnetic nanoparticles. Note the linear effects at low field for the suspensions. The effects increase with increasing particle volume concentration f.

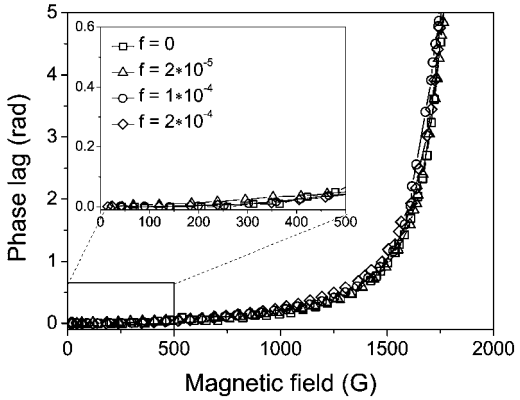

Fig. 3 The phase lag as a function of the magnetic field, for pure nematic and α-hematite nano-rod colloidal suspension cells. Within experimental error, all results fall on a single curve.

3. Theory

3.1 Model

We consider a ferronematic cell of thickness D with a rigid planar anchoring of the liquid crystal on the cell substrates (Fig. 1b). The model we develop is based on the continuum theory developed by Burylov and Raikher,[4] as modified by Zadorozhnii.[12,14] The liquid crystal matrix and the ferroparticle orientation are respectively characterized by the nematic director $\vec{n}(r)$, and by the magnetic director $\vec{m}(r)$, a unit vector in the direction of the ferroparticle magnetic moments. The appropriate free energy density for the complete system is:

$$F = \frac{1}{2}[K_1(\vec{\nabla}\cdot\vec{n})^2 + K_2(\vec{n}\cdot\vec{\nabla}\times\vec{n})^2 + K_3(\vec{n}\times\vec{\nabla}\times\vec{n})^2] - \frac{1}{2}\chi_a(\vec{n}\cdot\vec{H})^2 - fM_s(\vec{m}\cdot\vec{H}) - f\Omega(\vec{n}\cdot\vec{m})^2, \quad (2)$$

with K_1, K_2, K_3, respectively, the liquid crystal splay, twist and bend elastic constants, χ_a the anisotropy of the diamagnetic susceptibility, f the ferroparticle volume fraction, M_s the ferroparticle magnetization, and Ω the coupling energy density between the ferroparticle and the liquid crystal orientations. The first term represents the usual Frank-Oseen bulk energy density of the elastic deformations of nematic liquid crystal, the second term is the (direct) anisotropic part of the nematic liquid crystal magnetic energy, the third term represents the dipolar interaction between the ferroparticles and the magnetic field, while the final term determines the ferroparticle–liquid crystal interaction.

In the experimental system, the ferroparticle concentration is small, $f \sim 10^{-5}$–10^{-4}, which corresponds to an interparticle distance of the order of 10–50 particle diameters. The inter-ferroparticle interaction can thus be neglected, as these effects would only be included in higher order terms in a virial expansion. We also assume that the particles are uniformly distributed within the sample bulk. Thus we can also neglect the effect of particle aggregation and segregation.[1,15,21]

The effect of a magnetic field on the liquid crystal matrix in a ferronematic suspension can now be regarded as the sum of two distinct phenomena. On the one hand, there is a direct effect, associated with the molecular diamagnetic anisotropy, that is described by the second term in eqn (2). On the other hand, there is also an indirect effect, associated with the presence of ferromagnetic nanoparticles. This effect is driven by the third term in eqn (2) and acts on the liquid crystal director as a result of the magnetic–nematic coupling described by the fourth term in this equation.

In the recent theoretical studies of ferronematic systems,[12,14] the direct effect of the magnetic field was neglected. The resulting calculations might be regarded as applicable in the low external magnetic field limit, but in the very strong indirect coupling regime. In the low field limit the direct effect is always small as a result of the low liquid crystal diamagnetic susceptibility. However, our experimental data is not consistent with the theory of refs 12 and 14. For example, we observe an effective Frederiks transition and this is not predicted by their theory. Rather, the direct effect is dominant and the magnetic field-induced reorientation is only slightly perturbed by the presence of the colloidal particles. In order to overcome this problem here, we have specifically included the direct effect. We shall call our systems "weak ferronematics" systems. We note that, in principle, the model also treats the limit in which the indirect effect dominates ("strong ferronematics"), which is modeled also by refs 12 and 14.

We assume that the cell is uniform in the two in-cell plane directions, so that the nematic and magnetic directors depend only on the z coordinate. These quantities are respectively characterized by the angles $\theta(z)$ and $\psi(z)$ (Fig. 1b), where $0 < z < 1$ is the dimensionless coordinate scaled with the thickness D of the cell. Then the free energy functional reduces to:

$$F = \int_0^1 \frac{1}{2}\left(\frac{\mathrm{d}\theta}{\mathrm{d}z}\right)^2 [1 + p\sin^2\theta] - \frac{1}{2}[h\sin\theta + b\cos\theta]2 - \kappa[h\sin\psi + b\cos\psi] - \omega\cos^2(\psi - \theta)\,\mathrm{d}z, \quad (3)$$

where $p = (K_3 - K_1)/K_1$. The test magnetic field H is represented by the non-dimensional field $h = H/H_s$, where $H_s = D^{-1}\sqrt{K_1/\chi_a}$, and the bias magnetic field H_b is similarly scaled $b = H_b/H_s$. We note that the Frederiks threshold in the pure nematic at zero surface pre-tilt and zero bias field occurs at $h = \pi$.

The ferronematic system is characterized by the following two dimensionless parameters:

$$\kappa = \frac{M_s f D}{\sqrt{\chi_a K_1}}, \quad (4a)$$

$$\omega = \frac{\Omega f D^2}{K_1}. \quad (4b)$$

The *magnetic parameter* κ characterizes the ratio of the magnetic field effect on the ferroparticles to the direct coupling of the magnetic field with the nematic matrix. Thus $\kappa < 1$ and $\kappa > 1$ correspond respectively to the direct or indirect effects dominating the magnetic properties of the ferronematic suspension. The second parameter, ω, is the *coupling parameter*. In the Burylov–Raikher theory,[6] the other parameter $\omega_{BR} = W_s d/2K$ was used that scaled the surface anchoring coupling energy at a single particle with respect to the resulting elastic deformation energy. In the present model, following the notation of Zadorozhnii *et al.*, the coupling parameter ω (where $\Omega \sim W_s/d$) measures the coupling energy between nematic and magnetic orientations scaled to the deformation energy of the whole liquid crystal matrix.

It is reasonable to assume that both of the parameters are proportional to the colloidal ferroparticle concentration: κ characterizes the magnetic torque on the ferroparticles per unit volume and ω characterizes the consequent torque on the nematic director per unit volume, due to the ferroparticle–nematic coupling. The magnitude of these quantities can then be regarded as either a distinct theoretical problem, or an empirical question to be determined by experiment. In these circumstances, the proportionality of κ and ω to f is plausible but by no means necessary. This is the point of view we shall take in this paper.

3.2 Governing equations

The equilibrium state of the ferronematic system corresponds to the minimizer of the free energy functional given in eqn (3), with respect to the nematic orientation $\theta(z)$ and the magnetic orientation $\psi(z)$. Minimization yields the following Euler–Lagrange equations:

$$\frac{\mathrm{d}^2\theta}{\mathrm{d}z^2}[1 + p\sin^2\theta] + \left(\frac{\mathrm{d}\theta}{\mathrm{d}z}\right)^2 \frac{p}{2}\sin 2\theta + \frac{h^2 - b^2}{2}\sin 2\theta + hb\cos 2\theta + \omega\sin 2(\psi - \theta) = 0, \quad (5a)$$

$$\kappa(h\cos\psi - b\sin\psi) - \omega\sin2(\psi - \theta) = 0. \quad (5b)$$

This system of equations is solved with a Broyden non-linear solver,[22] using the method of successive iterations and a spectral method.[23] The small pre-tilt of the easy-axis on the cell substrates is taken into account as a fixed boundary condition for the solution: $\theta(z = 0, 1) = \alpha$. Thus, solving eqns (5a) and (5b) determines the nematic and magnetic director orientation angles $\theta(z)$ and $\psi(z)$, as a function of the test and bias magnetic fields h and b, pretilt angle α, and the specific ferronematic parameters κ and ω.

The pure nematic limit corresponds to $\kappa, \omega = 0$ in eqn (3). In this case eqns (5a) and (5b) decouple, eqn (5b) is identically satisfied and the functional depends only on $\theta(z)$. The relevant Euler–Lagrange equation then reduces to:

$$\frac{\mathrm{d}^2\theta}{\mathrm{d}z^2}[1 + p\sin^2\theta] + \left(\frac{\mathrm{d}\theta}{\mathrm{d}z}\right)^2 \frac{p}{2}\sin 2\theta + \frac{h^2 - b^2}{2}\sin 2\theta + hb\cos 2\theta = 0 \quad (6)$$

This equation is solved using the same procedure as above. The nematic director profile $\theta(z)$ inside the cell can be obtained for different magnetic field strengths h, b, and pre-tilt angles α.

We note also that for non-magnetic colloidal inclusions, $\kappa \to 0$, but $\omega \neq 0$. In this case eqns (5a) and (5b) decouple, the second equation gives $\theta = \psi$ and the nematic alignment is described by eqn (5a), exactly as for a pure liquid crystal. This is confirmed by the experimental results shown in Fig. 3 for the non-magnetic nanorods. Alternatively, the limit $\omega \to 0$, $\kappa \neq 0$,

corresponds to particles that may in themselves align, but whose alignment does not interact with the nematic director. Also, in this case, the nematic behaves like a pure liquid crystal.

4. Analysis of experimental data

4.1 Application of theoretical model

We now use the model described in the previous section to analyze the experimental data presented in Section 2.

The model prescribes the nematic director field $\theta(z)$ inside the nematic or ferronematic cell. The director field yields the local refractive indices $n_{e,o}$, where e, o denote the extraordinary and ordinary waves, respectively. The effective refractive index is defined by

$$n_{\mathrm{eff}} = n_{\mathrm{e}}[1 + \nu \sin^2\theta]^{-1/2}, \tag{7}$$

where $\nu = (n_{\mathrm{e}}^2 - n_{\mathrm{o}}^2)/n_{\mathrm{e}}^2$. The phase lag $\Delta\varphi$ between the ordinary and extraordinary polarization is given by:

$$\Delta\varphi = k_0 \int_0^1 (n_0 - n_{eff})\, \mathrm{d}z \tag{8}$$

where $k_0 = (2\pi D)/\lambda$, with λ as the wavelength of light in vacuo. The integral in eqn (8) can be computed using the Clenshaw–Curtis quadrature scheme.[23] The calculated value of the phase lag $\Delta\varphi$ determines the normalized cross-polarized intensity, $I_{\perp\,\mathrm{th}}$ (see eqn (1)). This can then be compared to the experimentally measured $I_{\perp\,\mathrm{exp}}$.

We have recently studied a detailed model of a nematic cell in a magnetic field with a small bias component.[24] In the presence of a small easy-axis pre-tilt, the presence of a bias field can induce a relatively large shift in the effective Frederiks threshold. It is impossible to obtain good agreement between the theory and experiment for both nematic and ferronematic cells without including both the bias field and the pre-tilt. In our comparison with the light transmission experiments, we take values for H_{b} and α directly from independent measurements.

The calculated dependence of $I_{\perp\,\mathrm{th}}(H)$ is fitted to the measured $I_{\perp\,\mathrm{exp}}(H)$. The fitting procedure finds fitting parameter values which minimize the mean square deviation between the calculated and experimental values. The goodness of fit is characterized by the normalized minimal deviation, r, defined by:

$$r = \frac{\sum (I_{\perp\,\mathrm{exp}} - I_{\perp\,\mathrm{th}})^2}{\sum I_{\perp\,\mathrm{exp}} \cdot I_{\perp\,\mathrm{th}}} \tag{9}$$

The fitting procedure is verified by analyzing the experimental data for the undoped nematic cell. The result is shown in Fig. 4. The cell thickness is known approximately, but its precise value $D = 49.2$ μm is determined from the zero-field cross-polarized intensity, $I_{\perp}(h = 0)$. The diamagnetic anisotropy χ_{a} is used as a fitting parameter, but all other parameters ($K_{1,3}$ and $n_{e,o}$) are taken from the literature. The best fit is obtained for $\chi_{\mathrm{a}} = 1.2 \times 10^{-7}$, a value consistent with those found in the literature.[20]

We now analyze the optical transmission data for the ferronematic cells, using the theory developed in Section 3. The extra fitting parameters are now only the magnetic and coupling parameters κ, ω. The cell thickness is again obtained from $I_{\perp}(h = 0)$, and the nematic diamagnetic anisotropy χ_{a} is not supposed to differ from that of the undoped liquid crystal. We can suppose that this is the case, because the nanorod-doped E7 (see Fig. 3) shows that the optical transmission – and hence presumably the nematic properties – are unaffected by doping at these low concentrations.

We tested three separate samples, with ferroparticle volume fractions of 2×10^{-5} (sample A), 1×10^{-4} (sample B) and 2×10^{-4} (sample C). In sample A, see Fig. 5, there is good agreement between the theory and the experiment giving an optimal fit, with the ferronematic parameters given by $\kappa = 0.08$, $\omega = 0.07$ (see Table 1).

In sample B, it is still possible to obtain a good fit between the model and the experiment, but this agreement holds only at low and intermediate magnetic fields, with the ferronematic parameters given by $\kappa = 0.31$, $\omega = 0.30$. These results are shown in Fig. 6. Above $H \approx 1800$ Gauss, the experimental and theoretical curves diverge. In particular, we note that the model predicts a set of oscillations of the normalized intensity $I_{\perp}$ which necessarily pass through zero and unity. On the other hand the maxima in the oscillations in the experimental data reach only about 0.5. This is a significant result, to which we shall return below.

This trend is confirmed in sample C, see Fig. 7. We can predict the general behavior of the system and obtain reasonable coupling parameter values: $\kappa \approx 0.5$ and $\omega \approx 0.4$. However, the oscillations exhibit a reduced amplitude and the fit at lower fields is not as good.

4.2 Discussion

The fitting parameters for the different samples are presented in Table 1 together with the goodness of fit parameter r. The coupling and magnetic parameters for ferronematic colloid for sample A ($f = 2 \times 10^{-5}$) are approximately four times smaller than those of sample B ($f = 1 \times 10^{-4}$). This is roughly consistent with the proportionality of these parameters to the ferroparticle concentration f predicted in eqns (4a) and (4b). However, this proportionality no longer holds for the higher concentration of $f = 2 \times 10^{-4}$.

The key theoretical equations, eqn (4a) and (4b), imply that the ratio κ/ω should be independent of the concentration of the nanoparticles, and thus it should be the same for all of the samples. In spite of the poorer fit for sample C, this ratio does not differ significantly from the others (see Table 1). We use this ratio to evaluate Ω, the effective coupling energy density per particle between nematic and magnetic orientations:

$$\Omega = \frac{M_{\mathrm{s}}}{D}\,\frac{\omega}{\kappa}\left(\frac{K_1}{\chi_{\mathrm{a}}}\right)^{1/2}, \tag{10}$$

where all parameters are either known (K_1, M_{s}) or taken from the $f = 0$ fit (D, χ_{a}). These values have also been included in Table 1. The average value of the coupling energy is $\Omega = (4 \pm 0.4) \times 10^4$ erg cm^{-3}. The Burylov–Raikher theory[4,6] refers to the quantity $W_{\mathrm{s}} = \Omega d$, where d is the typical dimension of a colloidal nanoparticle. In this theory W_{s} is an effective surface anchoring energy at the surface of a ferroparticle.[4] In our samples $W_{\mathrm{s}} \approx 8 \times 10^{-2}$ erg cm^{-2}. This quantity is of the same order of magnitude as that estimated by Kopčanský *et al.*[13]

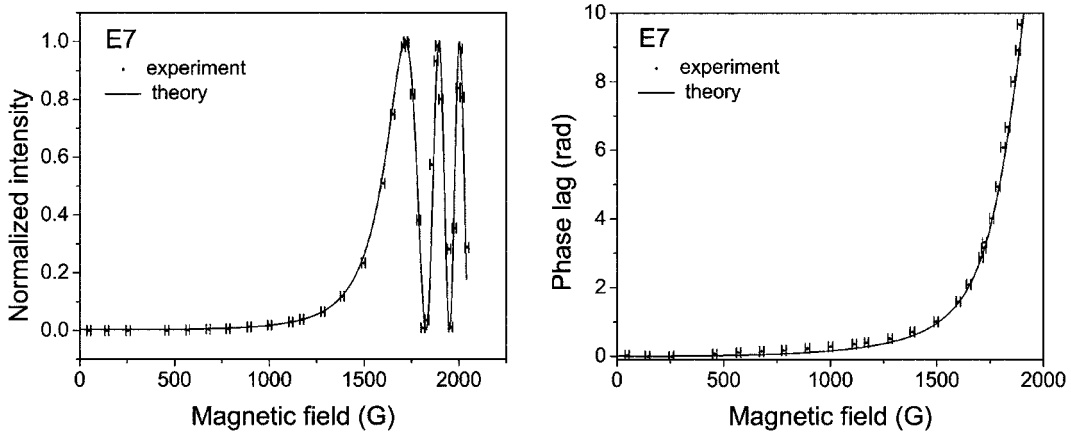

Fig. 4 The undoped liquid crystal E7 cell: the cross-polarized intensity and phase lag obtained from experiment (dots) and by numerical calculation using optimal parameters (solid line). Note that the error bars are horizontal rather than vertical, indicating that the uncertainty is in the applied field rather than the normalized intensity.

A more detailed examination of the data suggests that $\kappa \sim f^{0.84}$, and that $\omega \sim f^{0.75}$, with a good fit applying only to the κ data. These power laws are rather close, and might explain the observed rough constancy of the imputed Ω. At this stage, the evidence for a fractional power law depends on rather sparse data. In our view, if confirmed, the fractional power law suggests that aggregates form, possibly with fractal structure, and that the properties of the colloid depend sensitively on them.

The poorer fit of the theory to the data for larger values of f is reflected in the larger values of the goodness of fit parameter r. We note that r is of the same order of magnitude in the pure sample and sample A, and we have good confidence that a Frank–Oseen theory applies for the pure system. Both the power law behavior and the poorer fits at higher f are evidence that, while the basic physics is well described by the theory (*i.e.* magnetic coupling on the ferroparticles, steric coupling between the ferroparticles and the nematic), the detailed physics goes beyond the present theory.

We have two more pieces of preliminary evidence concerning this extra physics. The first concerns a remeasuring of the data for samples A–C after a delay of six months. In previous experiments,[25] it was noted that samples were stable for a six month time scale. In our case, measurements repeated after a six month interval showed the same general trends for all of the cells, but the values of the coupling parameters had changed by approximately 20%. Further aggregation that may have taken place over the six month interval could be one of the causes of the observed changes.

Table 1 Values of the magnetic and coupling parameters obtained from the fitting and estimation of the coupling energy for different samples

Suspension	r	κ	ω	κ/ω	Ω, erg cm^{-3}
Pure nematic	0.014	n/a	n/a	n/a	n/a
FN sample A	0.013	0.08	0.07	1.14	3.9×10^4
FN sample B	0.075	0.31	0.30	1.03	4.7×10^4
FN sample C	0.054	0.5	0.4	1.25	3.8×10^4

In Fig. 8 we show microscopy images of the three samples in zero field taken six months after preparing the cell. Sample A appears uniform, but large aggregates (~10–100 μm) are

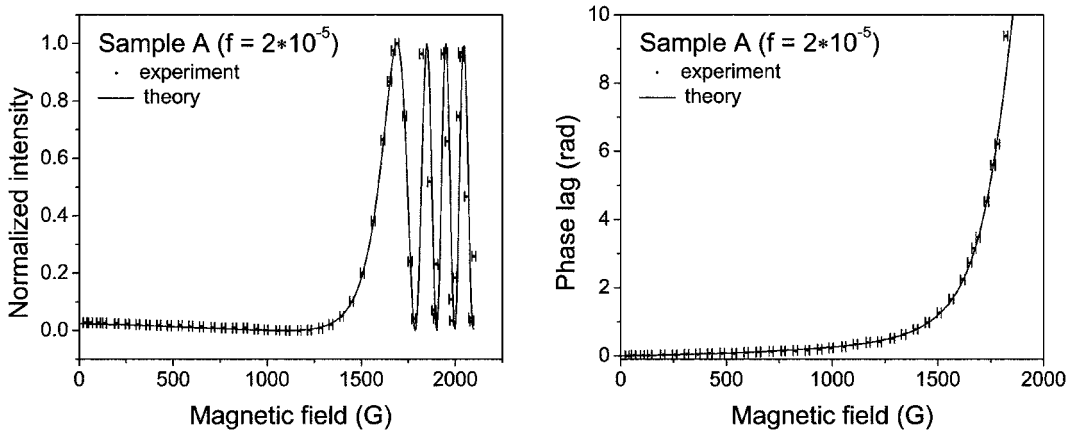

Fig. 5 Sample A, $f = 2 \times 10^{-5}$: optimal model predictions (solid line) and experimental values (dots) for the cross-polarized intensity $I_\perp$ and the phase lag. Note the good agreement between the model and the experiment, even up to high magnetic fields.

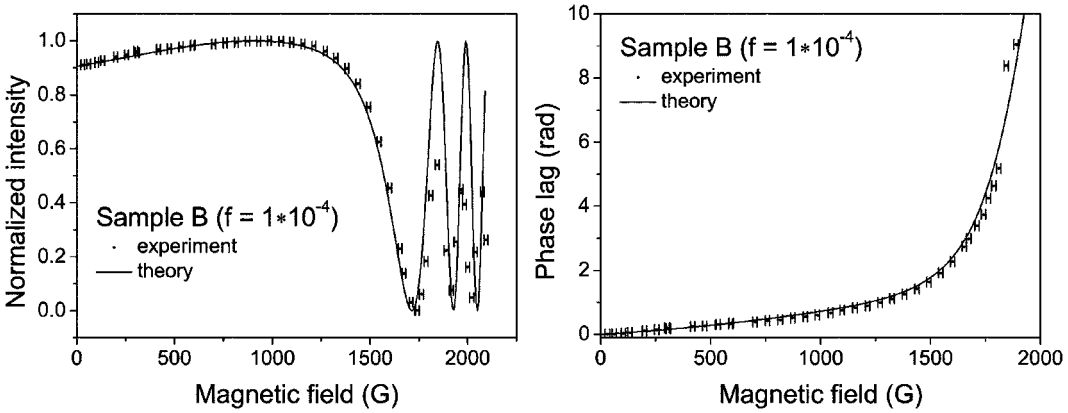

Fig. 6 Sample B, $f = 1 \times 10^{-4}$: optimal model predictions (solid line) and experimental values (dots) for the cross-polarized intensity $I_{\perp}$ and the phase lag. Note the good agreement between the model and the experiment holds only up to magnetic fields of ~1800 Gauss.

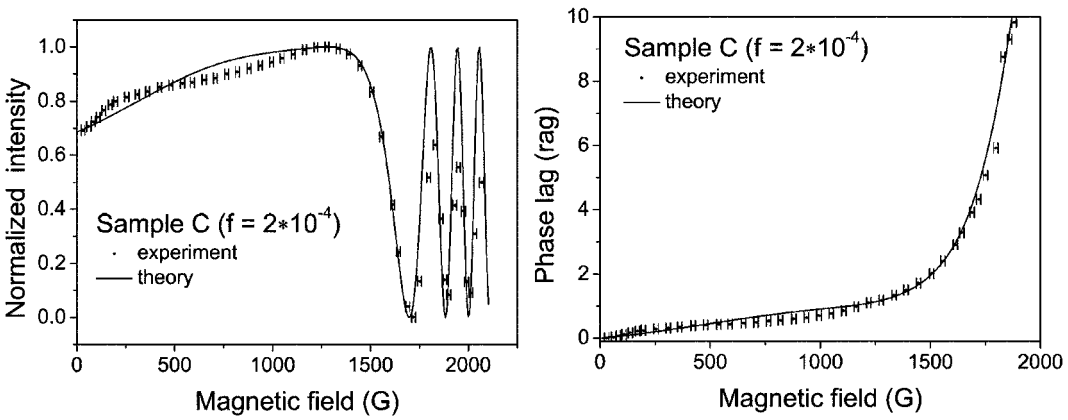

Fig. 7 Sample C, $f = 2 \times 10^{-4}$: optimal model predictions (solid line) and experimental values (dots) for the cross-polarized intensity $I_{\perp}$ and the phase lag. Note the only moderate agreement between the optimal model and the experimental curves, with poorer fits occurring both in the low field and high field regimes.

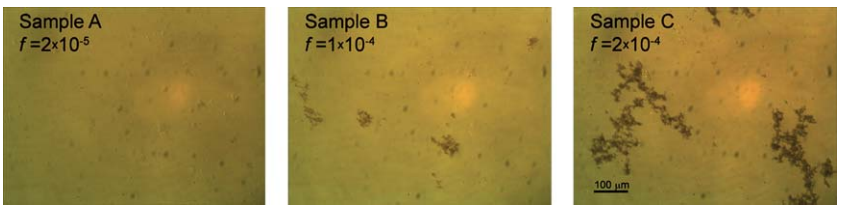

Fig. 8 Optical microscopy images of the cells containing samples A–C (from left to right).

observed in samples B and C. We conjecture that in our samples, the large aggregates are able to cause local distortion of the nematic director. The non-uniform director distortion would imply depolarization and scattering of the light passing through the cell. This, in turn, would lead to the drop in the oscillation amplitude of the measured intensity $I_{\perp \mathrm{exp}}$ observed in Figs. 6 and 7. The setup in the present experiment did not enable microscopy images to be obtained in the presence of the magnetic field, so this evidence is rather circumstantial. However, recent experiments of Buluy *et al.*[26] were able to investigate this, and indeed they did find hot spots around large aggregates.

5 Conclusion

In this paper we have reported a study of a ferromagnetic nanosuspension in a liquid crystal matrix. The study involved both optical transmission measurements and the development of a new theory to interpret the experiments. We have investigated the magnetic field-induced Frederiks transition in planar cells containing either the suspension or undoped nematic. Our samples are very weakly doped with nanoparticles (in the lowest case, one part in 50 000). Nevertheless, the suspensions show a detectable and unambiguous linear response to a magnetic field,

much lower than the Frederiks threshold in the undoped nematic. This response is approximately proportional to the ferroparticle concentration and is specifically the result of the fact that the particles are magnetic. Even at a low concentration, the suspension is sensitive to fields of the order of tens of Gauss units and is indeed promising for magnetically driven device applications.

Our experimental results cannot be explained by the previously developed theory of ferronematics, so in our approach we had to include the diamagnetic properties of the liquid crystals. This treats both the direct effect of the magnetic field, associated with the intrinsic magnetic properties of the liquid crystal, and an indirect effect, related to the magnetic properties of the nanoparticles. The model can, in principle, describe the magneto-optic response of ferronematics in the limits when either direct or indirect effects dominate. The model was fitted to the experimental data by choosing the values of two coupling parameters, κ and ω. The values of these parameters permitted us to determine the effective coupling energy density between the nematic and ferroparticle orientation.

Our model shows a good quality fit to the lowest concentration ($f = 2 \times 10^{-5}$) data. At higher concentrations, while we observe some deviation between the theory and the experiment, the theory still predicts the basic trend in the system. There are also hints of aggregation phenomena, whose interpretation may require more sophisticated theoretical treatment, which could be an obstacle to device applications. To provide more complete answers to these questions, however, will require further experimental investigation.

6. Acknowledgments

We thank Keith Daly for help with software development and Victor Zadorozhnii and Victor Reshetnyak for useful discussions. Financial support for this work was provided by CoI MOD, Royal Society UK-Ukraine Joint Project, and Science and Technology Center of Ukraine grant 5205. We are also particularly grateful to the referees who pointed out the importance of ref. 6.

References

1 F. Brochard and P. G. de Gennes, *J. Phys. (Paris)*, 1970, **31**, 691–708.
2 S.-H. Chen and N. M. Amer, *Phys. Rev. Lett.*, 1983, **51**, 2298–2301.
3 B. J. Liang and S.-H. Chen, *Phys. Rev. A: At., Mol., Opt. Phys.*, 1989, **39**, 1441–1446.
4 S. V. Burylov and Y. L. Raikher, *Phys. Rev. E: Stat. Phys., Plasmas, Fluids, Relat. Interdiscip. Top.*, 1994, **50**, 358–376.
5 S. V. Burylov and Y. L. Raikher, *J. Magn. Magn. Mater.*, 1993, **122**, 62–65.
6 S. V. Burylov and Y. L. Raikher, *Mol. Cryst. Liq. Cryst.*, 1995, **258**, 107–122 and 123–141.
7 V. Berejnov, J.-C. Bacri, V. Cabuil, R. Perzynski and Y. Raikher, *Europhys. Lett.*, 1998, **41**, 507–512.
8 Y. L. Raikher and V. I. Stepanov, *J. Magn. Magn. Mater.*, 1999, **201**, 182–185.
9 O. Buluy, E. Ouskova, Y. Reznikov, A. Glushchenko, J. West and V. Reshetnyak, *Mol. Cryst. Liq. Cryst.*, 2002, **375**, 81–87.
10 A. N. Zakhlevnykh, *J. Magn. Magn. Mater.*, 2004, **269**, 238–244.
11 P. Kopčanský, I. Potočova, M. Koneracká, M. Timko, A. G. M. Jansen, J. Jadzyn and G. Czechowski, *J. Magn. Magn. Mater.*, 2005, **289**, 101–104.
12 V. I. Zadorozhnii, A. N. Vasilev, V. Y. Reshetnyak, K. S. Thomas and T. J. Sluckin, *Europhys. Lett.*, 2006, **73**, 408–414.
13 P. Kopčanský, N. Tomašovičová, M. Koneracká, V. Zavisova, M. Timko, A. Dzarova, A. Sprincova, N. Eber, K. Fodor-Csorba, T. Toth-Katona, A. Vajda and J. Jadzyn, *Phys. Rev. E: Stat., Nonlinear, Soft Matter Phys.*, 2008, **78**, 011702.
14 V. I. Zadorozhnii, T. J. Sluckin, V. Y. Reshetnyak and K. S. Thomas, *SIAM J. Appl. Math.*, 2008, **68**, 1688–1716.
15 D. V. Makarov and A. N. Zakhlevnykh, *Phys. Rev. E: Stat., Nonlinear, Soft Matter Phys.*, 2010, **81**, 051710.
16 P. Kopčanský, N. Tomašovičová, M. Timko, M. Koneracká, V. Závišová, L. Tomočo and J. Jadzyni, *J. Phys.: Conf. Ser.*, 2010, **200**, 072055.
17 I. Dzyaloshinsky, *J. Phys. Chem. Solids*, 1958, **4**, 241–255.
18 R. Kotitz, W. Weitschies, L. Trahms and W. Semmler, *J. Magn. Magn. Mater.*, 1999, **201**, 102–104.
19 K. Y. Han, T. Miyashita and T. Uchida, *Jpn. J. Appl. Phys.*, 1993, **32**, L277–L279.
20 P. G. de Gennes and J. Prost, *The Physics of Liquid Crystals*, Clarendon Press, Oxford, 2nd edn, 1993.
21 S. B. Chernyshuk, B. I. Lev and H. Yokoyama, *J. Exp. Theor. Phys.*, 2001, **93**, 760.
22 C. G. Broyden, *Math. Comput.*, 1965, **19**, 577–593.
23 L. N. Trefethen, *Spectral Methods in Matlab*, SIAM, Philadelphia, 2000.
24 N. Podoliak, O. Buchnev, G. D'Alessandro, M. Kaczmarek and T. J. Sluckin, *Phys. Rev. E: Stat., Nonlinear, Soft Matter Phys.*, 2010, **82**, 030701R.
25 O. Buluy, E. Ouskova, Y. Reznikov and P. Litvin, *Ukr. J. Phys.*, 2004, **49**, A48–A50.
26 O. Buluy, S. Nepijko, V. Reshetnyak, E. Ouskova, V. Zadorozhnii, A. Leonhardt, M. Ritschel, G. Schönhense and Y. Reznikov, *Soft Matter*, 2011, **7**, 644–649.